$J/\psi \rightarrow$ vector + pseudoscalar decays and the quark content of η and η'

J. Jousset, Z. Ajaltouni, A. Falvard, H. Jnad, B. Michel, and J. C. Montret
Laboratoire de Physique Corpusculaire, Université de Clermont II, BP 45, F-63170 Aubière, France

D. Bisello, G. Busetto, A. Castro, L. Pescara, F. Racioppi, P. Sartori, and L. Stanco
Dipartimento di Fisica dell'Università di Padova, Istituto Nazionale di Fisica Nucleare, Sezione di Padova, I-35131 Padova, Italy

J. E. Augustin, G. Cosme, F. Couchot, F. Fulda, G. Grosdidier, B. Jean-Marie, V. Lepeltier, F. Mane, and G. Szklarz
Laboratoire de l'Accélérateur Linéaire, Université de Paris-Sud, F-91405 Orsay, France

R. Baldini and M. Schioppa
Laboratori Nazionali di Frascati dell'Istituto Nazionale di Fisica Nucleare, CP 13, I-00044 Frascati, Italy

(DM2 Collaboration)
(Received 5 June 1989)

Branching ratios of J/ψ decays into $\omega\pi^0, \omega\eta, \omega\eta', \rho\eta, \rho\eta', \phi\eta, \phi\eta'$, and $K^*(892)\bar{K}$ + charge conjugate are measured from the 8.6×10^6 J/ψ's produced by the DM2 experiment at the Orsay e^+e^- storage ring DCI. The η and η' mesons are found consistent with a $q\bar{q}$ structure and a mixing angle $\theta_P=(-19.1\pm1.4)°$.

I. INTRODUCTION

Interest in studies of the η and η' structures has been recently renewed by two-photon and J/ψ results. The pseudoscalar mixing angle θ_P and the ratio R_P of the wave function at the origin for the singlet η^1 and the octet η^8 states have been deduced from the width measurements of π^0, η, η' decays into $\gamma\gamma$.

The experimental values[1] $\theta_P=(-18.4\pm1.1)°$ and $R_P=0.94\pm0.02$ are hardly consistent with the nonet-symmetry assumption $R_P=1$ and the linear mass formula ($\theta_P=-23°$) and disagree with the quadratic-mass-formula value ($\theta_P=-10°$). Better consistency is found by assuming first-order correction in chiral perturbation theory. In such a picture[2] one obtains $R_P=0.97\pm0.02$, $\theta_P=(-22.7\pm1.1)°$, and $\theta_P=-19.5°$ for the linear and quadratic mass formulas, respectively.

Measurements of the hadronic decays $J/\psi\rightarrow$ vector + pseudoscalar provide information on the quark content of the η and η' mesons. If only connected diagrams [Figs. 1(a)–1(c)] are assumed to contribute, a large fraction of the η' content is accounted for by a gluonic component or a mixing with other pseudoscalars.[3] On the other hand it has been pointed out[4] that the amplitude of the disconnected diagrams [Fig. 1(d)], which may not be negligible, would allow to couple $q\bar{q}$ flavor singlet or glue component to the singlet part ω^1 of the vector nonet. Recent results[5] have indicated that the η and η' are consistent with being solely composed of light and strange quarks if the contribution of the disconnected diagrams is 15% of the connected ones.

This paper presents the results obtained with the DM2 detector from 8.6×10^6 J/ψ decays produced by the Orsay e^+e^- storage ring DCI. After a brief description of the apparatus in Sec. II, the analysis of the $J/\psi\rightarrow$ vector + pseudoscalar channels are reported in Sec. III. In Sec. IV the theoretical framework is described and the results on the quark composition of the η, η' mesons are given.

II. EXPERIMENTAL SETUP

The DM2 detector, described in detail elsewhere,[6] is a large-solid-angle magnetic spectrometer: a 2-m-diameter and 3-m-long solenoid with $1X_0$ aluminium coil produces a 0.5-T magnetic field. Inside the coil 2 proportional and 13 drift chambers allow the detection of charged particles over a solid angle of $0.87\times4\pi$ sr, with a momentum reso-

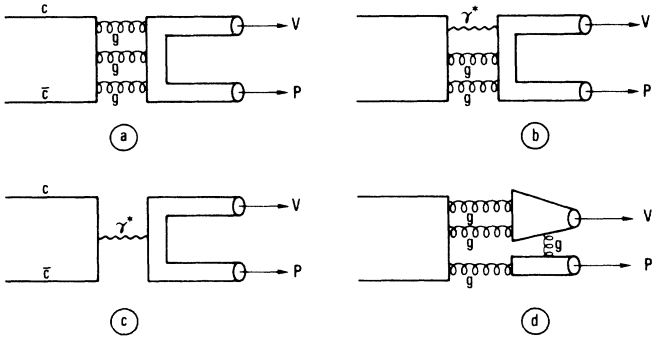

FIG. 1. Connected diagrams (a)–(c); disconnected diagrams (d).

lution of 3.5% at 1 GeV/c. A set of 36 2-cm-thick scintillators provides time-of-flight measurement with a total resolution of 540 ps, including 440 ps from the beam spread, and allows a 3σ π/K separation up to 450 MeV/c.

Outside the coil a photon detector ($5X_0$), divided into 8 octants of 14 planes of streamer tubes sandwiched with lead and scintillator planes, covers a solid angle of $0.7\times 4\pi$ sr with a detection efficiency greater than 96% for $E_\gamma \geq 110$ MeV. The spatial resolution for the photon direction is 10 mrad in azimuth and 7 mrad in polar angle. Matching is performed between the charged tracks and the tracks reconstructed in the photon detector in order to distinguish the true photons from fake ones induced by π and K interactions in the coil or in the photon detector. The photon energy is measured by combining the information on the number of tube hits and the analog-to-digital-converter (ADC) signals. The resolution scales as $0.19/\sqrt{E}$ (GeV) below 300 MeV and stays at the level of 35% above 300 MeV.

Two end-cap photon detectors, of $5X_0$ each, inside the magnetic field cover 12% of the solid angle. Because of the limited angular resolution and the lack of energy measurement this detector is used only as a veto to define the requested topology.

III. ANALYSIS

The topologies used in the study of the $J/\psi \rightarrow$ vector + pseudoscalar decays are shown in Table I. Some common analysis procedures are here described. All the decays have been searched for among events having the right number of charged tracks coming from a common vertex within the fiducial region along the beam axis, a zero total charge and, if not especially mentioned, the right number of photons detected in the barrel. Topologies with one missing photon have also been accounted for, whenever it was possible, in order to increase the total statistics. The mass determination from time-of-flight measurement, whenever available, had to be compatible with the mass hypothesis at 2σ. Finally the events have been kinematically fit by imposing energy-momentum conservation and any relevant mass constraints. The photon energy measurement has been used only to perform kinematical fits in the four-photon final state, final states with less than four photons being enough constrained by photon direction measurements. Moreover only photons with a measured or calculated energy greater than 20 MeV have been taken into account.

Efficiencies and analysis cuts have been determined from Monte Carlo[7] simulations according to the suitable dynamical hypotheses.

All the measured branching ratios are reported in Table II. Systematic errors account for normalization and efficiency uncertainties.

A. $J/\psi \rightarrow \omega\eta', \omega\eta, \omega\pi^0$ ($\omega \rightarrow \pi^+\pi^-\pi^0$)

1. $J/\psi \rightarrow \omega\eta'$ ($\eta' \rightarrow \pi^+\pi^-\eta$)

Events with four charged tracks and four photons have been selected[8] and four-constraint (4C) fit ($\chi^2 < 20$) by imposing the energy-momentum conservation. At this level, no η signal is present in the $\gamma\gamma$ invariant-mass distribution. A 5C fit has been performed by imposing a π^0 mass to one $\gamma\gamma$ pair and the combination having the lowest χ^2 has been chosen ($\chi^2 \leq 20$). The invariant mass of the two photons besides the π^0 exhibits (Fig. 2) a small but clear η signal having the expected mass resolution, showing evidence of $J/\psi \rightarrow \pi^+\pi^-\pi^+\pi^-\pi^0\eta$ production.

The η signal being observed, the 4C-selected events have been processed through a new 5C fit, by imposing

TABLE I. Decays of the pseudoscalar mesons and topologies of $J/\psi \rightarrow$ vector + pseudoscalar decays. For K^*K the indicated decays correspond to the final state.

Vector meson	Pseudoscalar meson	Decay		Topology
ρ	π^0	$\gamma\gamma$	(99%)	2C 2γ
($\pi^+\pi^-$)	η	$\pi^+\pi^-\pi^0$	(24%)	4C 2γ
		$\gamma\gamma$	(39%)	2C 2γ
	η'	$\eta\pi^+\pi^-$	(44%	4C 4γ
		$\rho\gamma$	(30%)	4C 1γ
ω	π^0	$\gamma\gamma$	(88%)	2C 4γ
($\pi^+\pi^-\pi^0$)	η	$\pi^+\pi^-\pi^0$	(21%)	4C 4γ
		$\gamma\gamma$	(35%)	2C 4γ
	η'	$\eta\pi^+\pi^-$	(40%)	4C 4γ (η in $\gamma\gamma$)
		$\rho\gamma$	(27%)	4C 3γ
ϕ	η	$\pi^+\pi^-\pi^0$	(12%)	4C 2γ
(K^+K^-)		$\gamma\gamma$	(19%)	2C 2γ
	η'	$\eta\pi^+\pi^-$	(22%)	4C 2γ (η in $\gamma\gamma$)
		$\rho\gamma$	(15%)	4C 1γ
$K^{*\pm}$	$K^\mp$	$K^\mp(K^\pm\pi^0)$	(33%)	2C 2γ
		$K^\mp(K_S^0\pi^\pm)$	(33%)	4C (K_S^0 in $\pi^+\pi^-$)
K^{*0}	K_S^0	$K_S^0(K^\pm\pi^\mp)$	(66%)	4C
		$K_S^0(K_L^0\pi^0)$	(17%)	(K_S^0 in $\pi^+\pi^-$)

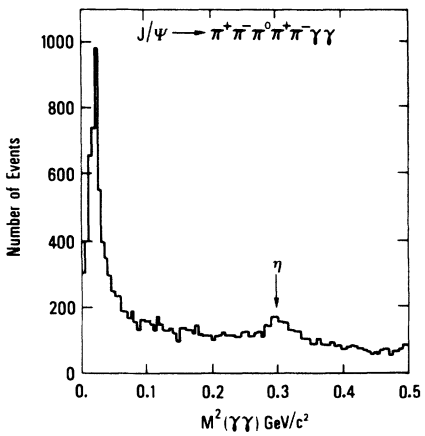

FIG. 2. Invariant mass squared of the two photons opposite to a π^0 for $J/\psi \rightarrow \pi^+\pi^-\pi^+\pi^-\pi^0\gamma\gamma$ events.

an η mass. The combination which gives the lowest χ^2 has been accepted if the squared invariant mass of the $\gamma\gamma$ pair not belonging to the η was smaller than 0.1 $(\text{GeV}/c^2)^2$. Finally the events have been given a 6C fit by imposing both η and π^0 masses ($\chi^2 < 20$).

The $\pi^+\pi^-\pi^0$ (Fig. 3) and $\pi^+\pi^-\eta$ mass [Fig. 4(a)] distributions of the selected events, four entries per event, give evidence of the ω and η' production, respectively. However, these productions are largely uncorrelated. Figure 4(b) shows the $\pi^+\pi^-\eta$ mass distribution when the opposite $\pi^+\pi^-\pi^0$ mass is compatible with the ω within 50 MeV/c^2: a small (six events) η' signal is present, well separated from the large production at higher mass. No event is observed at the η' mass when ω sidebands, $(m_\omega \pm 100) \pm 50$ MeV/c^2, are considered. The same result is obtained if η' bands are considered.

Background from incoherent $2(\pi^+\pi^-)\pi^0\eta$ production and from the $2(\pi^+\pi^-)3\pi^0$ decay has been found compatible with zero. Thus we calculate the following branching ratio for the $J/\psi \rightarrow \omega\eta'$ decay:

$$B(J/\psi \rightarrow \omega\eta') = (1.8^{+1.0}_{-0.8} \pm 0.3) \times 10^{-4} .$$

2. $J/\psi \rightarrow \omega\eta$ $(\eta \rightarrow \pi^+\pi^-\pi^0)$

Events from the $J/\psi \rightarrow \omega\eta$ channel, the η decaying into $\pi^+\pi^-\pi^0$, are expected to be also present into the sample of events used in the previous analysis (Fig. 2). Because of the large π^0 signal present in the $\gamma\gamma$ invariant mass, the events have been directly 6C fit ($\chi^2 < 20$) by imposing two π^0 masses. The lowest χ^2 combination has been retained.

The scatter plot of both $\pi^+\pi^-\pi^0$ masses (Fig. 5) shows a clean $J/\psi \rightarrow \omega\eta$ signal of 50 events with no background corresponding to the following branching ratio:

$$B(J/\psi \rightarrow \omega\eta) = (1.36 \pm 0.18 \pm 0.20) \times 10^{-3} .$$

3. $J/\psi \rightarrow \omega\eta(\eta \rightarrow \gamma\gamma)$; $J/\psi \rightarrow \omega\pi^0$

Events with two acollinear opposite charged tracks and four photons have been selected and given a 4C fit

TABLE II. Decay modes, final states, and branching ratios. The $\rho\pi$ branching ratio is a world-average value.

J/ψ decay mode	Final state	Branching ratio (10^{-3})
$\rho\pi$	$\pi^+\pi^-\pi^0$	13.2 ± 2.0
$\rho\eta$	$\pi^+\pi^-\gamma\gamma$	$0.200 \pm 0.050 \pm 0.030$
	$\pi^+\pi^-\pi^+\pi^-\pi^0$	$0.191 \pm 0.046 \pm 0.029$
	Average	$0.194 \pm 0.017 \pm 0.029$
$\rho\eta'$	$\pi^+\pi^-\gamma\rho^0$	$0.083 \pm 0.030 \pm 0.012$
$\omega\pi^0$	$\pi^+\pi^-\pi^0\pi^0$	$0.360 \pm 0.028 \pm 0.054$
$\omega\eta$	$\pi^+\pi^-\pi^0\gamma\gamma$	$1.45 \pm 0.11 \pm 0.21$
	$\pi^+\pi^-\pi^0\pi^-\pi^-\pi^0$	$1.36 \pm 0.18 \pm 0.20$
	Average	$1.43 \pm 0.10 \pm 0.21$
$\omega\eta'$	$\pi^+\pi^-\pi^0\pi^+\pi^-\eta$	$0.18^{+0.10}_{-0.08} \pm 0.03$
$\phi\eta$	$K^+K^-\gamma\gamma$	$0.58 \pm 0.06 \pm 0.10$
	$K^+K^-\pi^+\pi^-\pi^0$	$0.70 \pm 0.05 \pm 0.12$
	$K^+K^-\pi^+\pi^-\gamma$	$0.58 \pm 0.14 \pm 0.10$
	Average	$0.64 \pm 0.04 \pm 0.11$
$\phi\eta'$	$K^+K^-\pi^+\pi^-\eta$	$0.36 \pm 0.04 \pm 0.06$
	$K^+K^-\gamma\rho^0$	$0.45 \pm 0.05 \pm 0.08$
	Average	$0.41 \pm 0.03 \pm 0.08$
$K^{*+}K^- + \text{c.c.}$	$K^+K^-\pi^0$	$4.50 \pm 0.70 \pm 0.80$
	$K^0_S\pi^\pm K^\mp$	$4.58 \pm 0.17 \pm 0.69$
	Average	$4.57 \pm 0.17 \pm 0.70$
$K^{*0}\bar{K}^0 + \text{c.c.}$	$K^0_S K^0_L \pi^0$, $K^0 S K^0_S \pi^0$	$4.25 \pm 0.25 \pm 0.65$
	$K^0_S K^\pm \pi^\mp$	$3.85 \pm 0.15 \pm 0.58$
	Average	$3.96 \pm 0.15 \pm 0.60$

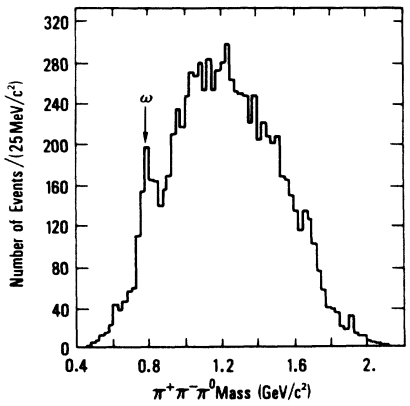

FIG. 3. $\pi^+\pi^-\pi^0$ mass distribution for $J/\psi \rightarrow \pi^+\pi^-\pi^+\pi^-\pi^0\eta$ events.

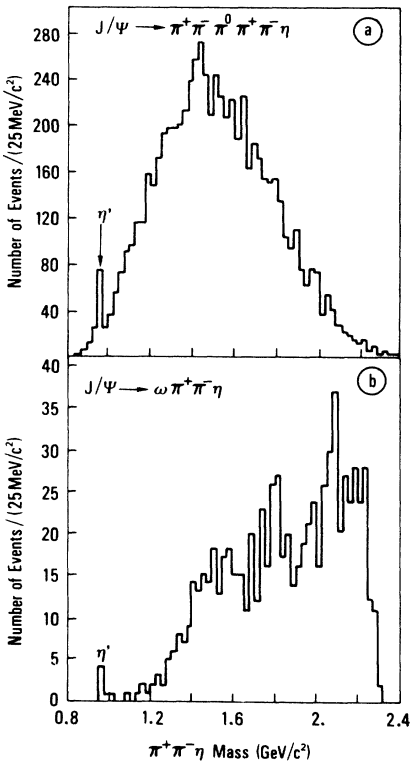

FIG. 4. $\pi^+\pi^-\eta$ mass distribution for $J/\psi \rightarrow \pi^+\pi^-\pi^+\pi^-\pi^0\eta$ (a) and $J/\psi \rightarrow \omega\pi^+\pi^-\eta$ events (b).

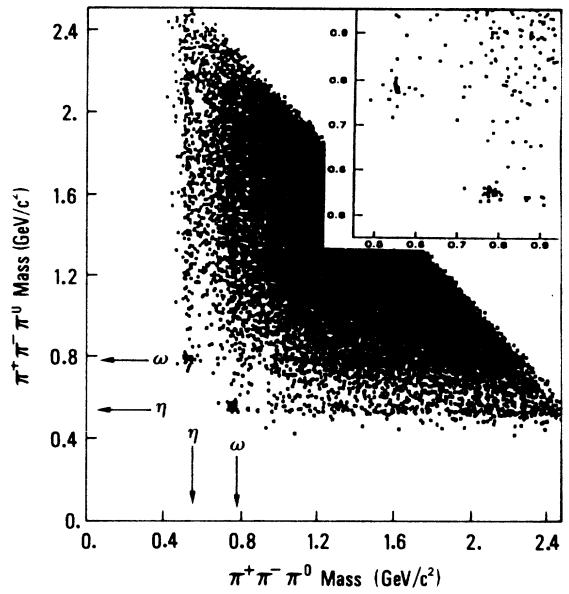

FIG. 5. Scatter plot $\pi^+\pi^-\pi^0$ mass versus $\pi^+\pi^-\pi^0$ mass for $J/\psi\to\pi^+\pi^-\pi^0\pi^+\pi^-\pi^0$ events.

($\chi^2\leq 20$). Owing to the large value of the π^0 (or η) momentum opposite to the ω (1446 and 1394 MeV/c, respectively), $J/\psi\to\omega\pi^0$ and $J/\psi\to\omega\eta$ events are characterized by a strong correlation between the ω and the π^0 (or η) signals. Both decays are seen (Fig. 6) in the mass scatter plot of the $m_{\pi^+\pi^-\gamma\gamma}$ versus the recoiling $m_{\gamma\gamma}$ mass when $m_{\gamma\gamma}$ is the highest $\gamma\gamma$ pair momentum. The distribution of the highest $\gamma\gamma$ momentum [Fig. 7(a)] shows two peaks at the expected values. In order to improve the $\gamma\gamma$ momentum resolution, the events have been 5C fit by imposing a π^0 mass constraint and accepted if the χ^2 of the best-fit combination was less than 20. Figure 7(b) shows the distribution of the highest momentum between the π^0 and the nonconstrained $\gamma\gamma$ pair for all the selected events and for the events whose recoiling mass is consistent with the ω within ± 50 MeV/c^2.

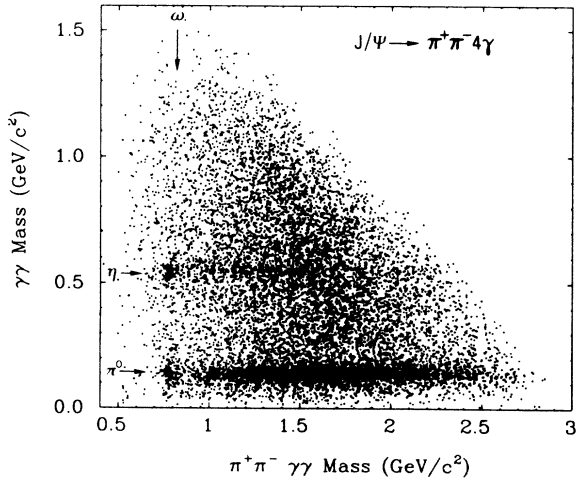

FIG. 6. $\pi^+\pi^-\gamma\gamma$ mass versus the $\gamma\gamma$ recoiling mass with higher momentum for $J/\psi\to\pi^+\pi^-\gamma\gamma\gamma\gamma$ events.

The number of $\omega\pi^0$ (222±19) and $\omega\eta$ (328±26) events has been found by fitting the $\gamma\gamma$ momentum distribution for all events of Fig. 7(b) to two Gaussian Breit-Wigner folded curves added to a polynomial background. The experimental resolutions, $\sigma=4.5\pm0.5$ and 5.4 ± 0.6 MeV/c, agree with the Monte Carlo expectations. Quite consistent results are obtained if the $\gamma\gamma$ momentum distribution recoiling against the ω [Fig. 7(b), shaded] is considered. The following branching ratios are determined:

$$B(J/\psi\to\omega\pi^0)=(3.60\pm0.28\pm0.54)\times10^{-4}\ ,$$

$$B(J/\psi\to\omega\eta)=(1.45\pm0.11\pm0.21)\times10^{-3}\ .$$

The events having five or six photons have been separately selected and processed through a parallel analysis. No extra background contribution has been found.

B. $J/\psi\to\rho\pi$

This channel is used to normalize the J/ψ production. Its branching ratio is more than 1% and a set of stringent cuts have been applied to isolate a clean sample of such decays. Events with two oppositely charged tracks and two or three photons are selected. Photon converted in

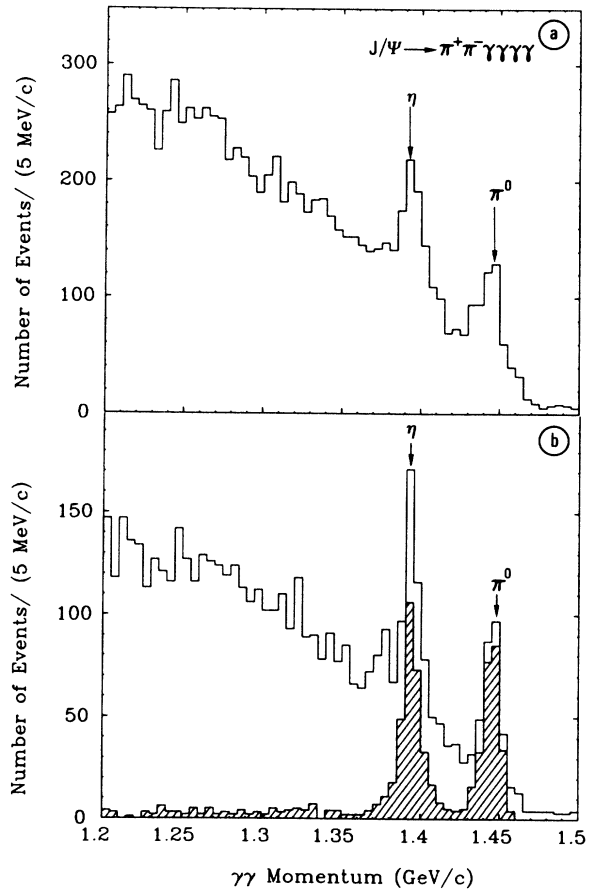

FIG. 7. $\gamma\gamma$ higher-momentum distribution for $J/\psi\to\pi^+\pi^-\gamma\gamma\gamma\gamma$ (a) and $J/\psi\to\pi^+\pi^-\pi^0\gamma\gamma$ events (b). The shaded distribution corresponds to the events with $m_{\pi^+\pi^-\gamma\gamma}$ in the ω band.

the vacuum pipe are eliminated by requiring that the angle between the two charged tracks be larger than 10°. An acoplanarity cut requires that the angle between the plane defined by two photons and the missing momentum be less than 7°. In order to improve the photon selection, the angle between two photons must be greater than 4° in space and 2.5° in the plane transverse to the beams. Radiative events are eliminated by requiring that the angle between a photon and a charged track be larger than 10°.

Then the events are fit to the $\pi^+\pi^-\gamma\gamma$ hypothesis. Each two-photon combination is tried and the event is retained if the lowest χ^2 is lower than 12. Finally the $\pi^+\pi^-\pi^0$ events are selected if $m^2_{\gamma\gamma} < 24\,000$ (MeV/c^2)^2. At this level two main sources of background remain. Fakes photons can contribute to transfer events from the 2C 1γ to the 2C 2γ topology. If the event was a real 2C 2γ with one undetected photon the fit with a fake photon may be successful. However these events are easily removed by cutting on the photon angle in the π^0 rest frame ($\cos\theta_\gamma < 0.98$). The other main contribution comes from the $J/\psi \to K^+K^-\pi^0$ channel. A large fraction of the events is eliminated by fitting the events to this hypothesis and by requiring $\chi^2_{\pi^+\pi^-\pi^0} < \chi^2_{K^+K^-\pi^0}$. The remaining contribution is then evaluated by Monte Carlo simulation and amounts to 460±87 events.

The total number of $\pi^+\pi^-\pi^0$ events after background subtraction is 21 435. The Dalitz plot (Fig. 8) shows that this channel is strongly dominated by the $\rho\pi$ dynamics. With an efficiency of (19.1±0.5)% and assuming for the branching ratio $J/\psi \to \rho\pi$ a world weighted average value[9] equal to $(1.3+0.2)\times 10^{-2}$, the total number of J/ψ produced is estimated to be $(8.6\pm 1.3)\times 10^6$.

C. $J/\psi \to \rho\eta$

1. $J/\psi \to \rho\eta\,(\eta \to \pi^+\pi^-\pi^0)$

Events with four charged tracks and one or two showers have been selected. Moreover the total charged momentum must be larger than 80 MeV/c. A 2C fit and a 1C fit imposing a missing π^0 mass to the 4C 2γ and 4C 1γ events, respectively, have been performed.

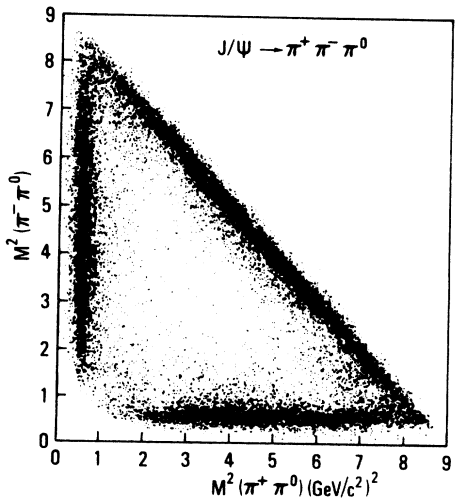

FIG. 8. Dalitz plot of $J/\psi \to \pi^+\pi^-\pi^0$ events.

The $m_{\pi^+\pi^-}$ versus $m_{\pi^+\pi^-\pi^0}$ scatter plot (four entries per event) gives evidence of associated $\rho\eta$ production [Fig. 9(a)]. Figure 9(b) shows the η signal when the invariant mass of the recoiling two pions is consistent with the ρ mass within ±150 MeV/c^2. Thus the $\pi^+\pi^-\eta$ events have been isolated by requiring $|m_{\pi^+\pi^-\pi^0} - m_\eta| \le 30$ MeV/c^2 for at least one mass combination. The invariant mass distribution of the remaining $\pi^+\pi^-$ pair is shown in Fig. 10(a). The observed events in the ρ mass region can be produced by both $J/\psi \to \rho\eta$ and $J/\psi \to \omega\eta \to \pi^+\pi^-\eta$ decays. Their respective contributions have been estimated by fitting the $\pi^+\pi^-$ mass distribution of Fig. 10(a) to the function

$$F(m_{\pi^+\pi^-}) = |A_\rho(m_{\pi^+\pi^-}) + A_\omega(m_{\pi^+\pi^-})e^{i\phi}|^2 + \text{linear background} .$$

A_ρ and A_ω are represented by Breit-Wigner functions up to a numerical factor:

$$A_V(m_{\pi^+\pi^-}) = \sqrt{N_V}F_{\mathrm{BW}_V}(m_{\pi^+\pi^-}) \quad (V \equiv \omega,\rho) .$$

The $\omega\eta$ contribution, $N_\omega = 29\pm 5$ events, is calculated from the previously reported branching ratio of $J/\psi \to \omega\eta$. The fit gives $N_\rho = 169\pm 41\rho\eta$ events which correspond to the branching ratio

$$B(J/\psi \to \rho\eta) = (1.91\pm 0.46\pm 0.29)\times 10^{-4} .$$

The phase ϕ between the two amplitudes is found to be consistent with zero ($\phi = -0.08\pm 0.17$).

2. $J/\psi \to \rho\eta\,(\eta \to \gamma\gamma)$

The events are looked for in the $\pi^+\pi^-\gamma\gamma$ sample described in Sec. III B. The $\rho\eta$ candidates are selected by requiring, after the $\pi^+\pi^-\gamma\gamma$ fit, that the $\gamma\gamma$ invariant mass be consistent with the η mass $530 \le m_{\gamma\gamma} \le 590$

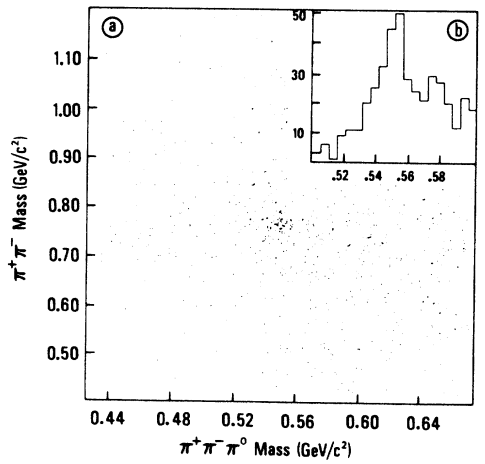

FIG. 9. $m_{\pi^+\pi^-}$ vs $m_{\pi^+\pi^-\pi^0}$ scatter plot, four entries per event, for $J/\psi \to \pi^+\pi^-\pi^+\pi^-\pi^0$ decays (a). The $m_{\pi^+\pi^-\pi^0}$ distribution for a recoiling pair with $|m_{\pi^+\pi^-} - m\rho| < 150$ MeV/c^2 (b).

MeV/c^2. No events are found in the η sidebands as expected from a Monte Carlo simulation of the $\rho\eta$ decay. The $\pi^+\pi^-$ invariant-mass distribution [Fig. 10(b)] fairly agrees with the corresponding distribution of the $\rho\eta$ events studied above [Fig. 10(a)]. The $\omega\eta$ and $\rho\eta$ contributions, $N_\omega = 12\pm3$ and $N_\rho = 130\pm31$, and the branching ratio

$$B(J/\psi\to\rho\eta) = (2.0\pm0.5\pm0.3)\times10^{-4}$$

are calculated in the same way as described in Sec. III C 1.

D. $J/\psi\to\rho\eta'\,(\eta'\to\rho\gamma)$

Four-charged-track events with one photon and a total charged momentum larger than 80 MeV/c have been 3C fit assuming four π masses. A ρ combination is selected by requiring

$$|m_{\pi^+\pi^-} - m_\rho| \le 150 \text{ MeV}/c^2 .$$

The invariant-mass distribution of the two remaining tracks shows clear evidence of a second ρ (Fig. 11). Events with two independent $\pi^+\pi^-$ masses satisfying the above condition have been selected, and the $\pi^+\pi^-\gamma$ mass has been computed (Fig. 12). A signal of 22 ± 7 events is observed at the η'.

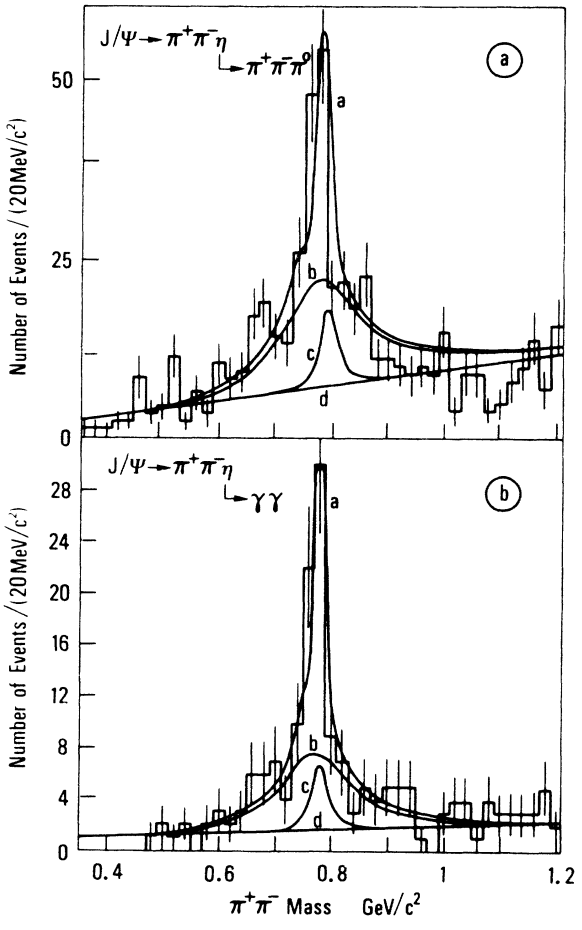

FIG. 10. $\pi^+\pi^-$ invariant mass of the $J\psi\to\pi^+\pi^-\eta$ events: $\eta\to\pi^+\pi^-\pi^0$ (a) and $\eta\to\gamma\gamma$ (b). The curves show the fit results for $\rho\omega$ interference term and background a, ρ, ω and background contributions b, c, d.

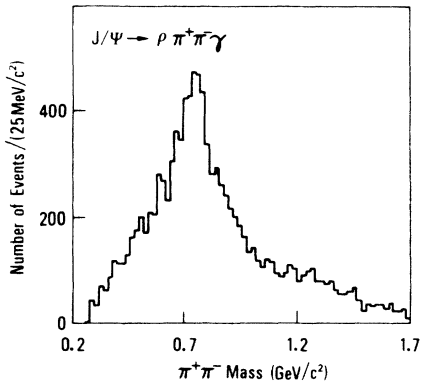

FIG. 11. $\pi^+\pi^-$ invariant mass opposite to a first ρ^0 for the $J/\psi\to\pi^+\pi^-\pi^+\pi^-\gamma$ events.

The number of $J/\psi\to\rho\eta'$ decays, $N_\rho = 19.2\pm7.5$, has been deduced from the total number N_T of $\pi^+\pi^-\eta'$ events, taking into account the interference effect with the $J/\psi\to\omega\eta'$ channel:

$$N_T = N_\rho + N_\omega + 2\left[\frac{\Gamma_\omega}{\Gamma_\rho}N_\rho N_\omega\right]^{1/2}\cos\phi .$$

The phase ϕ has been assumed to be zero as observed in the $J/\psi\to\rho\eta$ study and the $\omega\eta'$ contribution, $N_{\omega\eta'} = 0.8^{+0.5}_{-0.3}$ events, has been estimated from the branching ratio of Sec. III A 1. Then the branching ratio is

$$B(J/\psi\to\rho\eta') = (0.83\pm0.30\pm0.12)\times10^{-4} .$$

E. $J/\psi\to\phi\eta', \phi\eta$

1. $J/\psi\to\phi\eta'\,(\eta'\to\pi^+\pi^-\eta);\ J/\psi\to\phi\eta\,(\eta\to\pi^+\pi^-\pi^0)$

Events with four charged tracks and one or two pho-

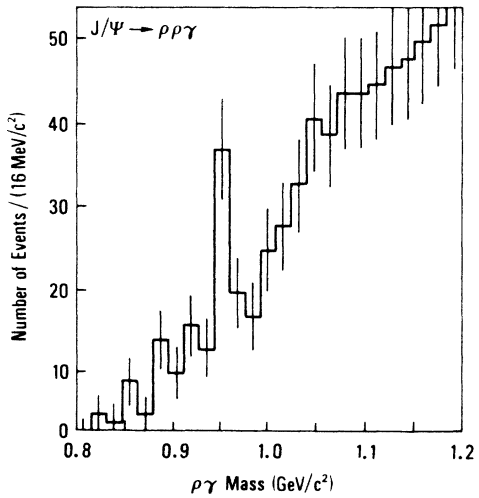

FIG. 12. $\rho\gamma$ invariant mass of the $J/\psi\to\rho^0\rho^0\gamma$ events.

tons have been selected. The ϕ has been looked for by computing the invariant mass $m_{K^+K^-}$ for each couple of oppositely charged tracks assuming kaon masses and selected by requiring

$$|m_{K^+K^-} - m_\phi| \leq 15 \text{ MeV}/c^2 .$$

The events have been 2C fit ($\chi^2 \leq 20$) assuming the two remaining particles to be pions. The scatter plot $m_{\pi^+\pi^-\gamma\gamma}$ versus $m_{\gamma\gamma}$ is shown in Fig. 13(a) for the selected events and in Fig. 13(b) for the ϕ sidebands. The decays $J/\psi \to \phi\eta$, $\eta \to \pi^+\pi^-\pi^0$, and $J/\psi \to \phi\eta'$, $\eta' \to \pi^+\pi^-\eta$, $\eta \to \gamma\gamma$, are evidenced. No relevant η or η' signal is observed in ϕ sidebands.

To improve the statistical significance of the $\phi\eta$, $\phi\eta'$ signals, events with one missing photon have also been considered. After the ϕ selection a 1C fit has been performed by requiring that the missing energy agrees with either a missing π^0 or a missing η.

The $\pi^+\pi^-\eta$ invariant mass of the events with one or two photons shows the η' signal near the phase-space limit over a low background (Fig. 14). The fit of this distribution gives $73\pm9\phi\eta'$ events from which the following branching ratio is deduced:

$$B(J/\psi \to \phi\eta') = (3.6\pm0.4\pm0.6)\times10^{-4} .$$

The analysis of the $J/\psi \to \phi\eta$ signal has been, for historical reasons, performed in a slightly different way. No preliminary ϕ selection has been applied and Fig. 15(a) shows the $\pi^+\pi^-\gamma\gamma$ mass distribution of the events selected by the 2C or 1C fit described above. The $m_{K^+K^-}$ mass distribution recoiling against the η, $|m_{\pi^+\pi^-\pi^0} - m_\eta| \leq 60$ MeV/c^2, gives evidence of the ϕ signal [Fig. 15(b)]. The fit of this distribution gives 169 ± 13 $\phi\eta$ events corresponding to

$$B(J/\psi \to \phi\eta) = (7.0\pm0.5\pm1.2)\times10^{-4} .$$

A third accumulation of events is present in the scatter plot of Fig. 13(a) which can be attributed to the $\eta(1280)$ or $f_1(1285)$. To estimate this signal only 4C 2γ events have been kept and the η has been selected by a cut on

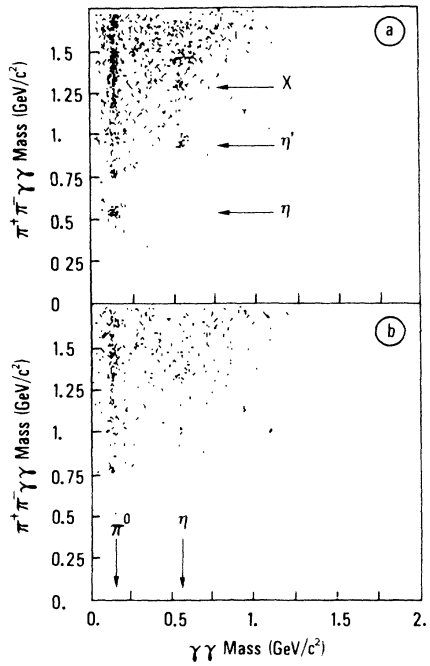

FIG. 13. $\pi^+\pi^-\gamma\gamma$ mass versus $\gamma\gamma$ mass for $J/\psi \to K^+K^-\pi^+\pi^-\gamma\gamma$ events with $m_{K^+K^-}$ in the ϕ band (a) and in the ϕ sidebands (b).

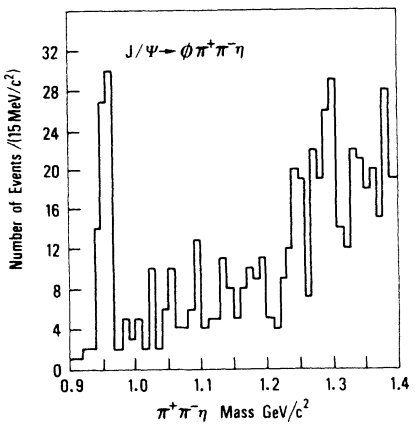

FIG. 14. $\pi^+\pi^-\eta$ invariant mass for $J/\psi \to \phi\pi^+\pi^-\eta$ events (4C 1γ and 4C 2γ topologies).

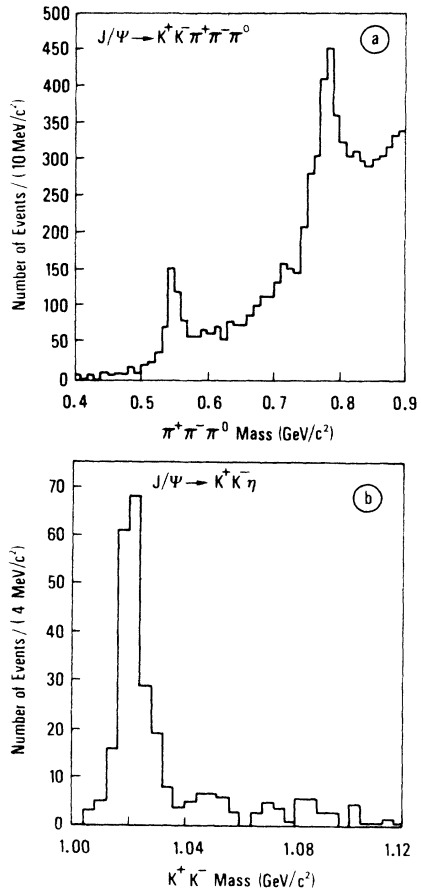

FIG. 15. $J/\psi \to K^+K^-\pi^+\pi^-\pi^0$: $\pi^+\pi^-\pi^0$ mass distribution (a) and K^+K^- mass opposite to the η (b).

the $\gamma\gamma$ invariant mass:

$$|m_{\gamma\gamma}-m_{\eta}| \leq 70 \text{ MeV}/c^2 .$$

A fit of the $\pi^+\pi^-\gamma\gamma$ invariant-mass distribution of Fig. 16(a) to two Breit-Wigner functions, the first one with the η' parameters, gives, for the second peak,

$$m = 1297\pm6 \text{ MeV}/c^2, \quad \Gamma = 10\pm8 \text{ MeV}/c^2$$

and 25 ± 6 events. No signal is observed in ϕ sidebands [Fig. 16(b)]. Therefore,

$$B(J/\psi\rightarrow\phi X(1297))\times B(X(1297)\rightarrow\eta\pi^+\pi^-) = (2.1\pm0.5\pm0.4)\times10^{-4}$$

A state is observed by DM2 at about the same mass in the J/ψ radiative decay into $\rho\pi^+\pi^-$ (Ref. 11) and $\eta\pi^+\pi^-$ (Ref. 12). Moreover a signal attributed to the $f_1(1285)$ is also present in ϕ-associated production of $4\pi^{\pm}$, $B(J/\psi\rightarrow\phi f_1(1285))=(3.2\pm0.6\pm0.4)\times10^{-4}$, and possibly $K_S^0K^{\pm}\pi^{\mp}$ (Ref. 13) final states.

2. $J/\psi\rightarrow\phi\eta\,(\eta\rightarrow\pi^+\pi^-\gamma)$; $J/\psi\rightarrow\phi\eta'\,(\eta'\rightarrow\rho\gamma)$

Events with four charged tracks and one photon have been selected and fit to the $K^+K^-\pi^+\pi^-\gamma$ hypothesis. Events with one additional photon which are incompatible with a fit to the $J/\psi\rightarrow K^+K^-\pi^+\pi^-\gamma\gamma$ hypothesis have been also included. These events have been analyzed as $J/\psi\rightarrow K^+K^-\pi^+\pi^-\gamma$ decays, both photons being successively included in the analysis. The combination giving the lowest χ^2 has been retained.

Figure 17(a) shows the scatter plot of the $\pi^+\pi^-$ versus the $\pi^+\pi^-\gamma$ invariant mass for ϕ events defined by $|m_{K^+K^-}-m_{\phi}| \leq 10 \text{ MeV}/c^2$. The $J/\psi\rightarrow\phi\eta'$, $\eta'\rightarrow\rho^0\gamma$ signal is clearly seen. The $\pi^+\pi^-\gamma$ mass distribution [Fig. 17(b)] shows the η' signal and the η contribution together with a broad distribution for the $\eta\rightarrow\pi^+\pi^-\pi^0$ decay with one undetected photon. No signal is observed into ϕ sidebands, defined by $10<|m_{K^+K^-}-m_{\phi}| \leq 20 \text{ MeV}/c^2$. Respectively, 20 ± 5 and 94 ± 10 events are observed for $J/\psi\rightarrow\phi\eta\rightarrow\phi\pi^+\pi^-\gamma$ and $J/\psi\rightarrow\phi\eta'\rightarrow\phi\pi^+\pi^-\gamma$ decays, corresponding to

$$B(J/\psi\rightarrow\phi\eta)=(5.8\pm1.4\pm1.0)\times10^{-4} ,$$

$$B(J/\psi\rightarrow\phi\eta')=(4.5\pm0.5\pm0.8)\times10^{-4} .$$

3. $J/\psi\rightarrow\phi\eta\,(\eta\rightarrow\gamma\gamma)$

The ϕ has been identified by its K^+K^- decay. Coplanarity has been imposed by a cut on the angle α of the missing-momentum direction with the plane of the two photons ($\alpha \leq 5°$). The events have been 2C fit in the $K^+K^-\gamma\gamma$ hypothesis ($\chi^2 \leq 7$). At this level the main background contribution comes from events having the correct topology but wrong mass assignment. They are eliminated if $\chi^2 \leq 7$ for at least one of the 2C fits in the $\pi^+\pi^-\gamma\gamma$ or $p\bar{p}\gamma\gamma$ hypothesis. The scatter plot $m_{K^+K^-}$ versus $m_{\gamma\gamma}$ is shown in Fig. 18(a) and the $m_{K^+K^-}$ invariant mass opposite to the η, $|m_{\gamma\gamma}-m_{\eta}| \leq 70 \text{ MeV}/c^2$, in

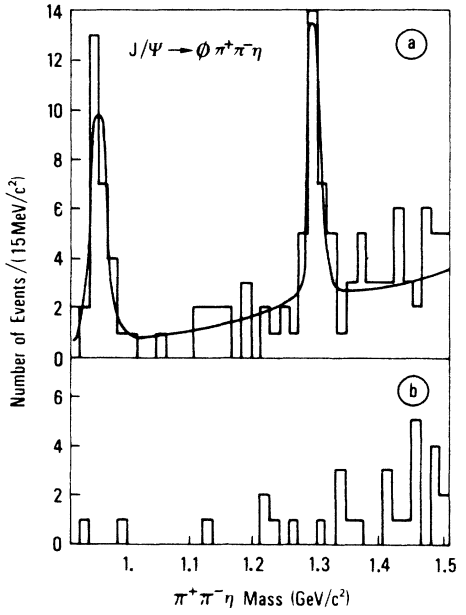

FIG. 16. $\pi^+\pi^-$ mass for $J/\psi\rightarrow\phi\pi^+\pi^-\gamma\gamma$ events with $m_{\gamma\gamma}$ in the η band (a) and η sidebands (b).

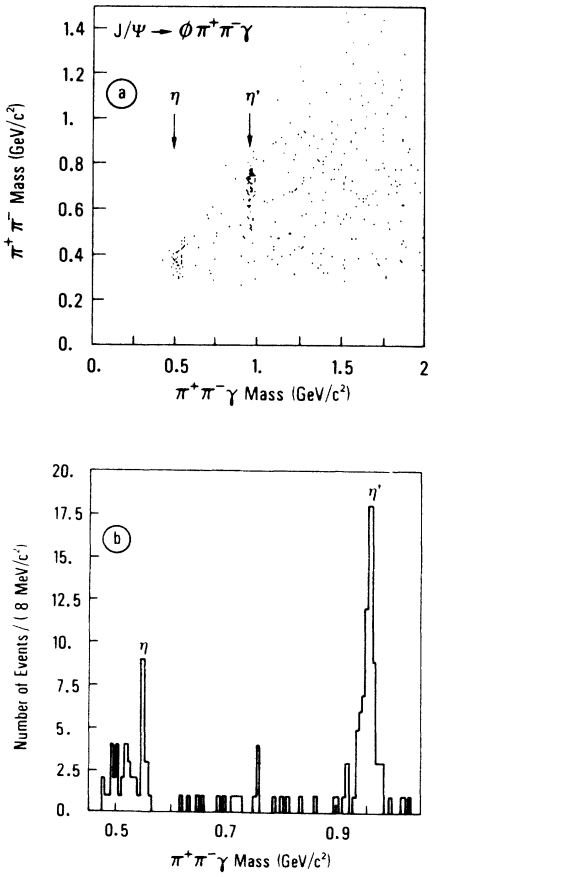

FIG. 17. $\pi^+\pi^-$ mass versus $\pi^+\pi^-\gamma$ mass of $J/\psi\rightarrow K^+K^-\pi^+\pi^-\gamma$ events (a) and $\pi^+\pi^-\gamma$ mass distributions of $J/\psi\rightarrow\phi\pi^+\pi^-\gamma$ events (b).

Fig. 18(b). The 157 ± 16 events lead to the branching ratio

$$B(J/\psi \to \phi\eta) = (5.8 \pm 0.6 \pm 1.0) \times 10^{-4} .$$

F. $J/\psi \to K^*(892)\bar{K} + \text{c.c.}$

1. $J/\psi \to K^{*0}\bar{K}^0 \to K_S^0 K_L^0 \pi^0$, $K_S^0 K_S^0 \pi^0$

Events with two oppositely charged tracks coming from a common vertex have been selected.[14] No requirement had been made on the vertex position and on the number of tracks in the photon detectors. The invariant mass in the two-pion hypothesis has to match the K^0 mass within 16 MeV/c^2. A cut on the invariant mass of the two charged particles, assuming pion and proton masses, $|m_{\pi p} - m_\Lambda| \leq 16$ MeV/c^2, rejects possible contaminations from channels with Λ's. Events are 1C fit by imposing the K^0 mass and rejected if $\chi^2 > 5$. The residual background is reduced by requiring a K_S^0 flight distance in the transverse plane within a range from 15 to 135 mm.

The K_S^0 momentum distribution (Fig. 19) shows the signal recoiling against the K^{*0} around 1370 MeV/c along with the signal recoiling against the K_L^0 at 1466 MeV/c. A fit to a Gaussian Breit-Wigner folded curve plus a Gaussian added to a polynomial background gives 403 ± 25 $K^{*0}K_S^0$ events. The K^{*0} decays into $K_L^0\pi^0$, $K_S^0(\to \pi^0\pi^0)\pi^0$ and, to a lesser extent, into $K^\pm\pi^\mp$ and $K_S^0(\to \pi^+\pi^-)\pi^0$ with both undetected charged tracks. Thus the following branching ratio is derived:

$$B(J/\psi \to K^{*0}\bar{K}^0 + \text{c.c.}) = (4.25 \pm 0.25 \pm 0.65) \times 10^{-3} .$$

This analysis gives also a measurement of the $J/\psi \to K_S^0 K_L^0$ branching ratio. Actually in the search for this decay other cuts based on the topology of the tracks in the photon detector have been applied in order to reduce the KK^* contribution. These cuts remove 16% of the $K_S^0 K_L^0$ and 65% of the $K_S^0 \bar{K}^{*0}$ signals in Fig. 19. The resulting branching ratio is

$$B(J/\psi \to K_S^0 K_L^0) = (1.18 \pm 0.12 \pm 0.18) \times 10^{-4} .$$

2. $J/\psi \to K^{*\pm}K^\mp \to K^+K^-\pi^0$

Events with two oppositely charged tracks and two photons have been selected. Candidates have been 3C fit to the $K^+K^-\pi^0$, $p\bar{p}\pi^0$, $\pi^+\pi^-\pi^0$ hypotheses and accepted if $\chi^2_{KK\pi} < 5$, $\chi^2_{p\bar{p}\pi}$ and $\chi^2_{3\pi} > 5$. Time of flight for each track, whenever available, had to be consistent with kaon assignment within 2.5σ.

The Dalitz plot of Fig. 20 shows the two K^* bands. The number of K^*K events, 2340 ± 50, is obtained by fitting the Dalitz-plot projections to Breit-Wigner curves added to a quadratic background. However a sizable contamination from $J/\psi \to \rho\pi$ remains in the data. Such events are indistinguishable from $J/\psi \to K^*K \to K^+K^-\pi^0$ and thus their contribution, $(40 \pm 8)\%$, has been calculated from Monte Carlo simulation and subtracted. Therefore the following branching ratio is set:

$$B(J/\psi \to K^{*\pm}K^\mp) = (4.5 \pm 0.7 \pm 0.8) \times 10^{-3} .$$

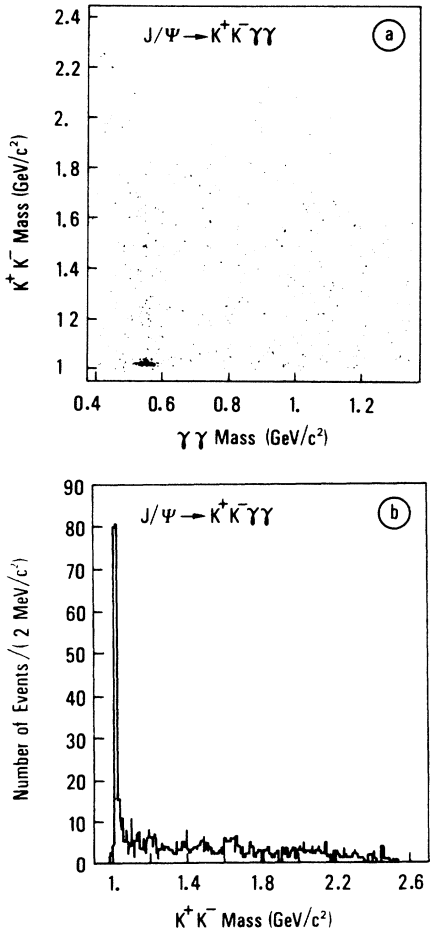

FIG. 18. K^+K^- mass vs $\gamma\gamma$ invariant mass of $J/\psi \to K^+K^-\gamma\gamma$ events (a) and K^+K^- mass opposite to the η for $J/\psi \to K^+K^-\eta$ events (b).

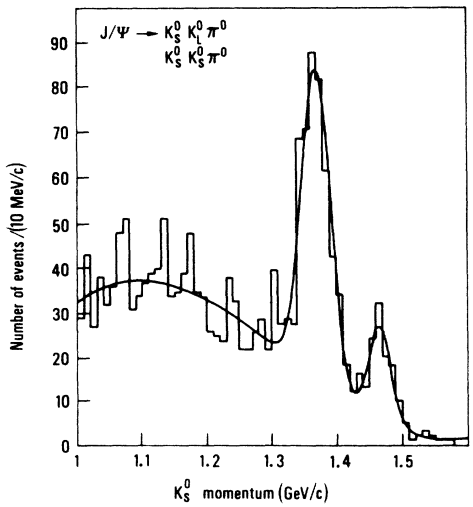

FIG. 19. K_S^0 momentum distribution of $J/\psi \to K_S^0 +$ neutrals after the K_S^0 flight cut.

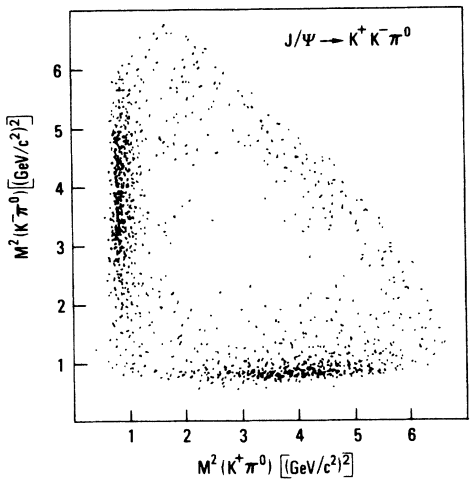

FIG. 20. Dalitz plot of $J/\psi \to K^+K^-\pi^0$ candidates.

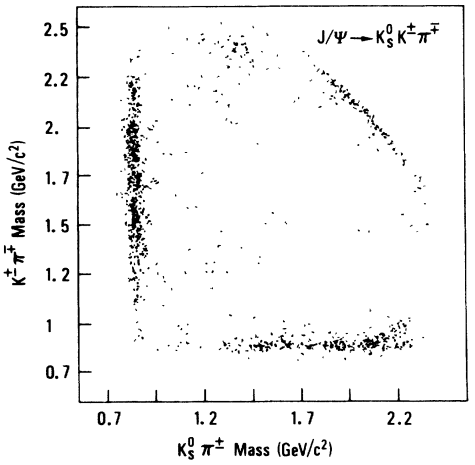

FIG. 21. $J/\psi \to K_S^0 K^{\pm}\pi^{\mp}$ events: $K_S^0\pi^{\pm}$ vs $K^{\pm}\pi^{\mp}$ mass distribution.

3. $J/\psi \to K^{*\pm}K^{\mp} + K^{*0}K^0 \to K_S^0 K^{\pm}\pi^{\mp}$

Events with four tracks, coming or not from a common vertex, are selected.[14] No requirement on the number of detected photons is made. Loose cuts on missing momentum $p_{\text{miss}} < 150$ MeV/c and on the reconstructed total energy in the four-pion hypothesis $E > 2500$ MeV reduce the background from $\pi^+\pi^- p\bar{p}$ and from channels with π^0's. A cut on the angle between any track pair is used to eliminate γ conversion in the beam pipe. Finally events are 3C fit by imposing momentum conservation ($\chi^2 < 10$).

The K_S^0 is selected by a cut on the invariant two-pion mass, $|m_{\pi^+\pi^-} - m_K| < 25$ MeV/c^2, when the two tracks come from a secondary vertex or $455 < m_{\pi^+\pi^-} < 530$ MeV/c^2 when no secondary vertex is found. At least one particle of the K_S^0 decay should have time-of-flight (TOF) measurement consistent with a pion mass within 2.5σ.

The selected events are 4C fit to the $\pi^+\pi^- K^{\pm}\pi^{\mp}$ hypothesis. Two $K\pi$ mass combinations being possible, TOF measurements, if they exist, must be consistent with 2.5σ with the mass hypotheses. If both combinations pass the TOF consistency cut, the combination giving the lowest χ^2 is retained.

The scatter plot of Fig. 21 shows the K^{*0} and $K^{*\pm}$ bands. The number of $K^{*\pm}K^{\mp}$, 881±31, and $K^{*0}K_S^0$, 789±30, events is obtained by fitting the plot projections onto the $K_S^0\pi^{\pm}$ and $K^{\pm}\pi^{\mp}$ mass axes to a Breit-Wigner curve added to a polynomial background. The resonance parameters are

$$m_{K^{*0}} = 894.8 \pm 1.4 + \text{MeV}/c^2 ,$$

$$\Gamma_{K^{*0}} = 52.6 \pm 3.6 \text{ MeV}/c^2 ,$$

$$m_{K^{*\pm}} = 889.0 \pm 1.6 \text{ MeV}/c^2 ,$$

$$\Gamma_{K^{*\pm}} = 56.2 \pm 4.3 \text{ MeV}/c^2 ,$$

and the following branching ratios are calculated:

$$B(J/\psi \to K^{*\pm}K^{\mp}) = (4.58 \pm 0.17 \pm 0.69) \times 10^{-3} ,$$

$$B(J/\psi \to K^{*0}\bar{K}^0 + \text{c.c.}) = (3.85 \pm 0.15 \pm 0.58) \times 10^{-3} .$$

IV. DISCUSSION

Parity conservation implies that the decay $J/\psi \to$ vector + pseudoscalar proceeds through P wave. Thus the decay amplitudes are simply related to the branching ratio for each final state by

$$B(J/\psi \to V + P) = |A|^2 \times p_V^3$$

in which p_V is the vector-meson momentum.

Taking into account the contributions from the 3-gluon and electromagnetic connected diagrams [Figs. 1(a)–1(c)] the amplitudes of the various decays can be expressed in terms of an SU(3)-symmetric strong amplitude A, and two additional amplitudes D and D' involving, respectively, electromagnetic and quark mass SU(3)-symmetry breaking.[15] The contribution of these various amplitudes can be evaluated through standard SU(3) calculations.[16]

We will use in the following the notation $g = A + 2D'$, $h = 3D'$, $e = D$ of Ref. 17. A phase ϕ between the elec-

TABLE III. Amplitudes assuming connected diagram dominance.

J/ψ decay mode	Amplitude (according to Ref. 16)	Amplitude (according to Ref. 17)
$\rho^{\pm}\pi^{\mp}$, $\rho^0\pi^0$	$A + D + 2D'$	$g + e$
$K^{*\pm}K^{\mp}$	$A - D' + D(2-x)$	$g - h + e(2-x)$
$K^{*0}K^0$	$A - D' - 2D(1+x)/2$	$g - h - 2e(1+x)/2$
$\omega\eta$	$(A + 2D' + D)X_\eta$	$(g + e)X_\eta$
$\omega\eta'$	$(A + 2D' + D)X_{\eta'}$	$(g + e)X_{\eta'}$
$\phi\eta$	$(A - 4D' - 2Dx)Y_\eta$	$(g - 2h - 2ex)Y_\eta$
$\phi\eta'$	$(A - 4D' - 2Dx)Y_{\eta'}$	$(g - 2h - 2ex)Y_{\eta'}$
$\rho^0\eta$	$3DX_\eta$	$3eX_\eta$
$\rho^0\eta'$	$3DX_{\eta'}$	$3eX_{\eta'}$
$\omega\pi^0$	$3D$	$3e$
$\phi\pi^0$	0	0

TABLE IV. Amplitudes assuming disconnected diagram contribution.

$\omega\eta$	$(g+e)X_\eta+\sqrt{2}rg(\sqrt{2}X_\eta+Y_\eta)$
$\omega\eta'$	$(g+e)X_{\eta'}\sqrt{2}rg(\sqrt{2}X_{\eta'}+Y_{\eta'})$
$\phi\eta$	$(g-2h-2ex)Y_\eta+r(g-h)(\sqrt{2}X_\eta+Y_\eta)$
$\phi\eta'$	$(g-2h-2ex)Y_{\eta'}+r(g-h)(\sqrt{2}X_{\eta'}+Y_{\eta'})$

tromagnetic amplitude D and the strong ones A and D' is also introduced, whereas A and D' are assumed to be real with respect to each other. The parameter x which accounts for the different electromagnetic coupling of s and u,d quarks has been fixed to 0.64 (Ref. 18). The amplitudes for the considered decays are given in Table III in both notations. In this table X_η, Y_η, $X_{\eta'}$, $Y_{\eta'}$ are defined by[19]

$$|\eta\rangle=\frac{X_\eta}{\sqrt{2}}|u\bar{u}+d\bar{d}\rangle+Y_\eta|s\bar{s}\rangle\ ,$$

$$|\eta'\rangle=\frac{X_{\eta'}}{\sqrt{2}}|u\bar{u}+d\bar{d}\rangle+Y_{\eta'}|s\bar{s}\rangle\ .$$

The parameter values are obtained by fitting[20] all the $J/\psi \to$ vector + pseudoscalar branching ratios of Table II. The results (Table VI, first column) show that, in the hypothesis of a dominance of connected diagrams, the η is saturated by its u, d, s quark content ($X_\eta^2+Y_\eta^2=0.99\pm0.12$) whereas this is not true for the η' ($X_{\eta'}^2+Y_{\eta'}^2=0.70\pm0.13$).

It has been suggested[4] that the η' result could be accounted for by a non-negligible contribution of disconnected diagrams.

Disconnected diagrams couple the vector meson to the singlet component of the pseudoscalar meson so enhancing the singlet part η^1 which is mainly η'. An additional parameter r, relative weight of the disconnected to connected diagrams, is included in the fit, and the conditions

$$X_\eta^2+Y_\eta^2=1,\quad X_{\eta'}^2+Y_{\eta'}^2=1$$

are imposed. The amplitudes in this hypothesis[21] are given in Table IV. The results (Table VI, second column) show that with a small contribution of disconnected diagrams (13±4)% the η and η' are saturated by their quark content.

Moreover the disconnected diagrams could couple also to a gluonic singlet content within the η' wave function. Such a coupling is introduced in the parametrization of the amplitude (Table V) taking, for the η' wave function,

$$|\eta'\rangle=\frac{X_{\eta'}}{\sqrt{2}}|u\bar{u}+d\bar{d}\rangle+Y_{\eta'}|s\bar{s}\rangle+Z_{\eta'}|G\rangle\ ,$$

where $|G\rangle$ stands for an unknown gluonic component. The results of this fit (Table VI, third column) show that

TABLE V. Amplitudes assuming a glue component coupled to the disconnected diagram.

$\omega\eta$	$(g+e)X_\eta$
$\omega\eta'$	$(g+e)X_{\eta'}+\sqrt{2}r(g-2h/3)/Z_{\eta'}$
$\phi\eta$	$(g-2h-2ex)Y_\eta$
$\phi\eta'$	$(g-2h-2ex)Y_{\eta'}+r(g-2h/3)Z_{\eta'}$

TABLE VI. Fit results. In hypothesis 1 only the connected diagrams contribute [$\chi^2=8.5$ for 2 degrees of freedom (DF)]. Hypothesis 2 includes the contribution of disconnected diagrams assuming $\chi_\eta^2+Y_\eta^2=1$ and $X_{\eta'}^2+Y_{\eta'}^2=1$ ($\chi^2=2.8$ for 3 DF). In hypothesis 3 a glue component Z is included with $X^2+Y^2+Z^2=1$ ($\chi^2=5.1$ for 2 DF).

	Hypothesis 1	Hypothesis 2	Hypothesis 3
g	0.979±0.063	1.030±0.041	0.985±0.051
h	0.086±0.064	0.134±0.038	0.095±0.049
e	0.117±0.004	0.116±0.004	0.117±0.004
ϕ	1.369±0.094	1.369±0.100	1.369±0.102
X_η	0.732±0.039	0.755±0.040	0.732±0.035
$X_{\eta'}$	0.335±0.063	0.514±0.054	0.529±0.065
$\lvert Y_\eta\rvert$	0.667±0.065	0.656±0.046	0.680±0.039
$Y_{\eta'}$	0.623±0.061	0.858±0.031	0.842±0.033
r		−0.108±0.018	−1.73±0.14
$Z_{\eta'}$			0.105±0.059

the gluonic part is very small, $|Z_{\eta'}|^2\sim1\%$. It is noticeable that in both fits r is negative so indicating a 180° phase between disconnected and connected diagram amplitudes. The same result has been already found in a previous study of the $J/\psi \to$ vector + tensor decays.[13]

Since the η and η' mesons are found to be consistent with pure $q\bar{q}$ systems if the disconnected diagram contribution is taken into account, the data have been further analyzed in the framework of the quark model to extract the value of the pseudoscalar mixing angle between η^1 and η^8. Then X_η, Y_η, $X_{\eta'}$, $Y_{\eta'}$ are expressed as a function of one of them, for instance,

$$Y_\eta=-\sqrt{1-X_\eta^2},\quad X_{\eta'}=-Y_\eta,\quad Y_{\eta'}=X_\eta\ .$$

Fitting the data with this free parameter one obtains $X_\eta=0.812\pm0.018$ from which the following value of the pseudoscalar mixing angle is inferred:

$$\sin\theta_P=1/\sqrt{3}(-\sqrt{2}X_\eta+\sqrt{(1-X_\eta^2)})=(-19.1\pm1.4)^\circ\ .$$

This result agrees with the same measurement by the Mark III Collaboration[5] and with the values obtained from the $J/\psi \to \gamma\eta,\gamma\eta'$ and the $\pi^0,\eta,\eta' \to \gamma\gamma$ decays and with the $\gamma\gamma$ experiments.[1,22] An exhaustive discussion of such results can be found in Ref. 23.

V. CONCLUSION

The branching ratios of J/ψ into $\rho\pi$, $\rho\eta$, $\rho\eta'$, $\omega\pi^0$, $\omega\eta$, $\omega\eta'$, $\phi\eta$, $\phi\eta'$, and $K^*(892)\bar{K}$ + c.c. have been measured from 8.6×10^6 J/ψ's. The obtained values agree with the latest Mark III results with the systematics.

The η, η' quark content has been studied by fitting the data to various phenomenological models. When including a contribution of disconnected J/ψ decays diagrams, the η, η' mesons are found to be consistent with pure $q\bar{q}$ system. The disconnected diagrams contribution amounts to (13±4)% of the connected amplitudes. The value of the pseudoscalar mixing angle between η^1 and η^8, $\theta_P=(-19.1\pm1.4)^\circ$, agrees with previous measurements.

The gluonic component in the η' wave function, if it exists, is found to be very small ($|Z_{\eta'}|^2 \simeq 1\%$).

Finally a measurement of the SU(3)-forbidden $J/\psi \to K_S^0 K_L^0$ decay is reported. Moreover in the ϕ-associated production of $\eta\pi\pi$ one observes clean production of a state which can identified with the $\eta(1280)$ or the $f_1(1285)$.

ACKNOWLEDGMENTS

We would like to thank the technicians of the DM2 group for the construction and maintenance of the apparatus, and the technical staff of the LAL for its constant support, especially the DCI storage ring group directed by P. Marin.

[1]J. Olsson, in *Lepton and Photon Interactions,* proceedings of the International Symposium on Lepton and Photon Interactions at High Energies, Hamburg, West Germany, 1987, edited by R. Rückl and W. Bartel [Nucl. Phys. B (Proc. Suppl.) **3**, 613 (1988)].

[2]J. Donoghue, B. Holstein, and Y. Lin, Phys. Rev. Lett. **55**, 2766 (1985).

[3]R. M. Baltrusaitis *et al.* Phys. Rev. D **32**, 2883 (1985).

[4]S. S. Pinski, Phys. Rev. D **31**, 1753 (1985).

[5]D. Coffman *et al.*, Phys. Rev. D **38**, 2695 (1988).

[6]J. E. Augustin *et al.*, Phys. Scr. **23**, 623 (1981).

[7]C. Amsler and J. C. Bizot, Comput. Phys. Commun. **30**, 21 (1983).

[8]The analyses of Secs. III A 1 and III A 2 are based on 6.1×10^6 J/ψ's.

[9]The branching ratio error is twice that reported in the most recent Particle Data Group review (Ref. 10). Our estimate has been used in all the previous DM2 analyses. On the other hand this value accounts also for all the systematics of the experiment not specially mentioned.

[10]Particle Data Group, G. P. Yost *et al.*, Phys. Lett. B **204**, 325 (1988).

[11]D. Bisello *et al.*, Phys. Rev. D **39**, 701 (1989).

[12]J.-E. Augustin *et al.*, Report No. LAL 88-59, 1988 (unpublished).

[13]A. Falvard *et al.*, Phys. Rev. D **38**, 2706 (1988).

[14]This analysis is based on 4.38×10^6 J/ψ's.

[15]The importance of SU(3)-breaking mechanisms in $J/\psi \to$ vector + pseudoscalar can be demonstrated by calculating, for instance, the ratio $B(J/\psi \to K^{*+}K^-)/B(J/\psi \to \rho^+\pi^-)$, whose experimental value is 0.34 ± 0.08 instead of 0.85.

[16]S. Rudaz, Phys. Rev. D **14**, 298 (1976); H. Kowalski and T. F. Walsh, *ibid.* **14**, 852 (1976); J. Pasupathy and C. A. Singh, *ibid.* **18**, 791 (1978).

[17]H. E. Haber and J. Perrier, Phys. Rev. D **32**, 2961 (1985).

[18]The effects of different electromagnetic contributions to the amplitudes can be evidenced by considering, for instance, the ratio $B(J/\psi \to K^{*0}\bar{K}^0 + \text{c.c.})/B(J/\psi \to K^{*\pm}K^{\mp})$, whose experimental value is 0.87 ± 0.06 instead of 1. However the value of x is weakly constrained by the fit.

[19]J. L. Rosner, Phys. Rev. D **27**, 1101 (1983).

[20]Actually in the fit procedures the Y_η parameters are assumed to be negative because of the measured values of θ_P and only $|Y_\eta|$ are constrained.

[21]A. Seiden, H. Sadrozinski, and H. Haber, Phys. Rev. D **38**, 824 (1988).

[22]DM2 has measured $J/\psi \to \gamma\eta, \gamma\eta'$ obtaining $\theta_P = (-21.9 \pm 1.3)°$. See F. Couchot, in *Searches for New and Exotic Phenomena,* proceedings of the Twenty-third Rencontre de Moriond, Les Arcs, France, 1988, edited by O. Fackler and J. Tran Thanh Van (Editions Frontières, Gif-sur-Yvette, 1988); thesis, Universite' de Paris-Sud, Report No. LAL 87-55.

[23]F. J. Gilman and R. Kauffman, Phys. Rev. D **36**, 2761 (1987).